

Pygmy Dipole Resonances: Nuclear and Coulomb Excitations

E.G. Lanza^{1,2}, **A. Vitturi**^{3,4}, **M.V. Andrés**⁵, **F. Catara**^{2,1},
D. Gambacurta^{2,1}

¹I.N.F.N. – Sezione di Catania, 95123 Catania, Italy

²Dipartimento di Fisica e Astronomia, 95123 Catania, Italy

³Dipartimento di Fisica, 35131 Padova, Italy

⁴I.N.F.N. – Sezione di Padova, 35131 Padova, Italy

⁵Departamento de Física Atomica, Molecular y Nuclear, 41080 Sevilla, Spain

Abstract. We study the nature of the low-lying dipole strength in neutron-rich nuclei, often associated to the Pygmy Dipole Resonance. The states are described within the Hartree-Fock plus RPA formalism, using different parametrizations of the Skyrme interaction. We analyze their nature and we show that they are not of collective nature although many particle-hole configurations participate in their formation. We show how the information from combined reactions processes involving Coulomb and different mixtures of isoscalar and isovector nuclear interactions can provide more hints to unveil the characteristic features of these states.

1 Introduction

Evidence of new phenomena associated with the increase of the neutron number in nuclei has been accumulated in recent years. [1]. Approaching the neutron dripline, a neutron skin develops, *i.e.* a concentration of neutron density partly decoupled from the core nucleons. Previous calculations [2] have shown that as soon as the neutron number increases, some strength appears at low energies in the dipole strength distribution, well below the dipole giant resonance. This strength, carrying few per cent of the isovector EWSR, is present in many nuclear isotopes and has been associated to the pygmy dipole resonances (PDR). Such a low-lying dipole strength has been widely studied within several microscopic models, among which we quote the Hartree-Fock plus Random Phase Approximation (RPA) with Skyrme interactions, the Relativistic RPA (RRPA) and the Relativistic Hartree Bogoliubov (RHB) plus the Relativistic Quasi particle RPA (RQRPA). For a recent bibliography see ref. [1]. Whether such strength corresponds (or not) to a collective mode is still under discussion.

From the experimental information, measurements involving high energy Coulomb excitation processes with heavy ion collisions have been performed at GSI on ^{132}Sn [3] as well as on ^{68}Ni [4]. Another well-established method to

study the PDR is by means of nuclear resonance fluorescence (or real photon-scattering experiments) performed on semimagic nuclei at Darmstadt [5]. Recently, the same nuclei have been investigated by means of the $(\alpha, \alpha'\gamma)$ coincidence method at KVI [6]. Further information on the PDR, both on theoretical and experimental investigation, can be found in N. Tsoneva's contribution to these proceedings.

The evidence for these states comes therefore essentially from Coulomb excitation processes which provide information only on the multipole $B(E\lambda)$ transition rates. If one wants to understand better the nature of these states one has to envisage different reactions which can provide further information on wave functions and transition densities. Part of this information can be obtained by resorting to reactions where the nuclear part of the interaction is also involved [7]. The relative role of the nuclear and Coulomb components, as well as of the isoscalar and isovector contributions, can be modified by choosing in an appropriate way the projectile mass, charge, bombarding energy and scattering angle of the reaction.

In this contribution we will first investigate the nature of the low lying dipole states and then show the predictions for the excitation of the low-lying (PDR) and high-lying (GDR) dipole states in the neutron-rich ^{132}Sn by different projectiles (α , ^{40}Ca , ^{48}Ca) at different bombarding energies. The analysis about the properties of PDR is carried out by means of a novel criterion aimed to study the features and the collectivity degree of the PDR. The semiclassical framework within which the inelastic cross section are calculated is briefly described. We will show how the excitation probabilities are sensitive to the details of the transition densities (and not simply to the $B(E1)$ values) and how these can be probed by combination of different processes.

2 The Nature of the PDR

The dipole states, their wave functions and the corresponding transition densities have been obtained within the Hartree-Fock plus discrete RPA with Skyrme interactions. As an example we show in Figure 1 the results for the strength distributions for the three isotopes $^{100,120,132}\text{Sn}$ [8]. The curves are generated by a smoothing procedure using a Lorentzian with a 1 MeV width. We observe the usual lowering of the energies of the dominant Giant Dipole Resonance with increasing mass number. As soon as the neutron number is increasing we notice the appearance of some low-lying strength (carrying a fraction of the EWSR of the order of few per cent) below 10 MeV. These are precisely the states that are candidates to be interpreted as Pygmy Dipole Resonances.

One important question is how collective these dipole states are. Several authors have taken as measure of the collectivity the number of particle-hole configurations entering in the RPA wavefunction with an appreciable weight [9, 10]. Such criteria do not take into account the other fundamental concept that underlies collectivity, *i.e.* the coherence. The reduced transition probability from

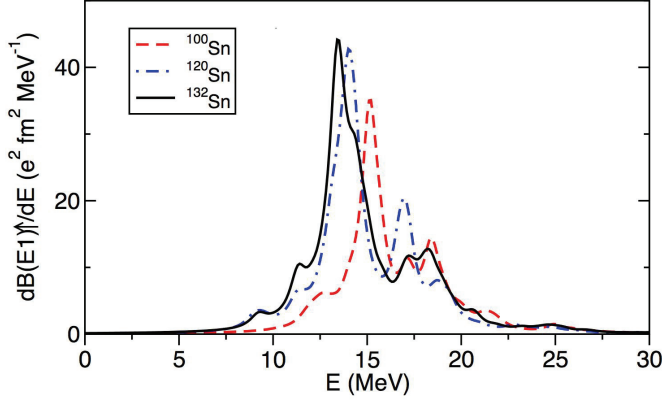


Figure 1. Isovector strength distributions for dipole states for tin isotopes calculated with the SGII interaction. The curves represent $dB(E1)/dE$ as obtained by adopting a smoothing procedure.

the ground state to the excited state ν can be written as

$$B(E\lambda) = \left| \sum_{ph} b_{ph}(E\lambda) \right|^2 = \left| \sum_{ph} (X_{ph}^\nu - Y_{ph}^\nu) T_{ph}^\lambda \right|^2 \quad (1)$$

where T_{ph}^λ are the 2^λ multipole transition amplitudes associated with the elementary p-h configurations. The previous analysis, based only on the relative magnitude of the X and Y RPA amplitudes, can be misleading because it does not take into account the matrix element T_{ph}^λ nor the relative signs of the separate contributions. Indeed, if we look also to the b_{ph} 's we note that configurations with a small percentage may give large contribution to the reduced transition probability [8]. In Figure 2 we plot the partial contributions b_{ph} versus the order number of the p-h configurations used in the RPA calculations for three states of the ^{132}Sn isotope. The bars corresponds to the individual values of the b_{ph} while the continuous thin line is the cumulative sum of the contributions. The dashed lines divide the protons from the neutron configurations. The order goes from the most bound configurations to the higher ones. The figure on the left is for the low-lying dipole state while the one in the middle is for the GDR state. For further comparison we plot also the results for the low-lying 3^- state. For the low-lying dipole states there are several p-h configurations participating to the formation of the $B(E1)$ but some of them have opposite sign giving rise to a final value which is small. For the other two states we have a different behaviour: one can clearly see how the $B(E\lambda)$ of the GDR and low lying 3^- states are built up by the small contributions of many p-h configurations which add coherently. From our novel analysis, it emerges that, although the low-lying dipole states cannot be considered as collective as the GDR states, they cannot be described as pure p-h configuration.

Pygmy Dipole Resonances: Nuclear and Coulomb Excitations

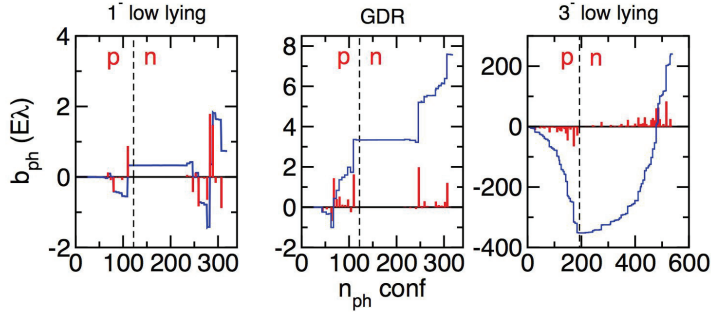


Figure 2. Partial contributions $b_{ph}(E\lambda)$, in units of $e^2 fm^{2\lambda}$, of the reduced transition probability vs. the order number of the p-h configurations used in the RPA calculations with the SGII interactions. The vertical dashed lines divide the protons from the neutron configurations. The order goes from the most to the less bound ones. The solid bars corresponds to the individual b_{ph} contributions while the unbroken thin line is the cumulative sum of the contributions. The figures on the left, middle and right correspond to the low lying dipole state, the GDR and to the low lying 3^- state, respectively.

More precise information on the specific nature of the states is contained in their transition densities. The RPA transition densities associated with the GDR (right frame) and with a state in the PDR region (left frame) in ^{132}Sn are shown in Figure 3. Neutron and proton components of the transition densities are separately shown, together with their isoscalar and isovector combinations. The two cases clearly display characteristics which are proper of different excitation modes. The one associated with the GDR shows the usual opposite-phase behaviour of the proton and neutron components, leading to a dominant isovector character. The situation is rather different in the case of the other state at lower energy. Here neutron and proton components seem to oscillate in phase in the interior region, while in the external region only the neutrons give a contribution to both isoscalar and isovector transition densities which have the same magnitude. Such behaviour, which has been found also in all the other microscopic approaches [11], can be taken as a sort of definition of PDR.

We are indeed in presence of a new mode which in the literature is often macroscopically described as the oscillation of the neutron skin with respect to the proton+neutron cores. A macroscopic description of such a mode assumes a separation of the neutron density into a core part ρ_N^C with N_C neutrons and a valence part ρ_N^V with N_V neutrons ($N = N_C + N_V$), with a proton density ρ_P with Z protons. This leads to neutron and proton transition densities given by

$$\begin{aligned} \delta\rho_N(r) &= \beta \left[\frac{N_V}{A} \frac{d\rho_N^C(r)}{dr} - \frac{N_C + Z}{A} \frac{d\rho_N^V(r)}{dr} \right] \\ \delta\rho_P(r) &= \beta \left[\frac{N_V}{A} \frac{d\rho_P(r)}{dr} \right] \end{aligned} \quad (2)$$

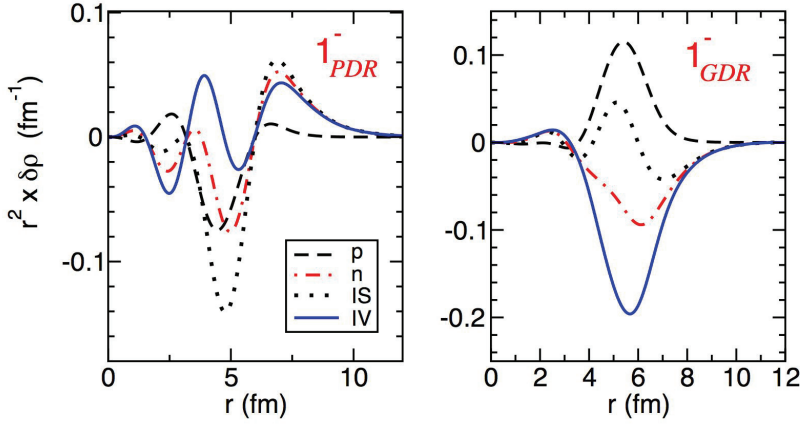


Figure 3. Transition densities for the low-lying dipole state (PDR) (left) and for the GDR (right) for the ^{132}Sn isotope calculated with the SLY4 interaction. We show the proton, neutron, isoscalar and isovector components (as indicated in the legend).

with β a proper strength parameter. The microscopic RPA and the macroscopic transition densities, normalized to the same $B(E1)$ value, are compared in Figure 4. Although some similarities are present, a full interpretation of the state in the above macroscopic terms is not obvious. It should be noted that, besides the requirement of the shape of the transition density, the macroscopic picture

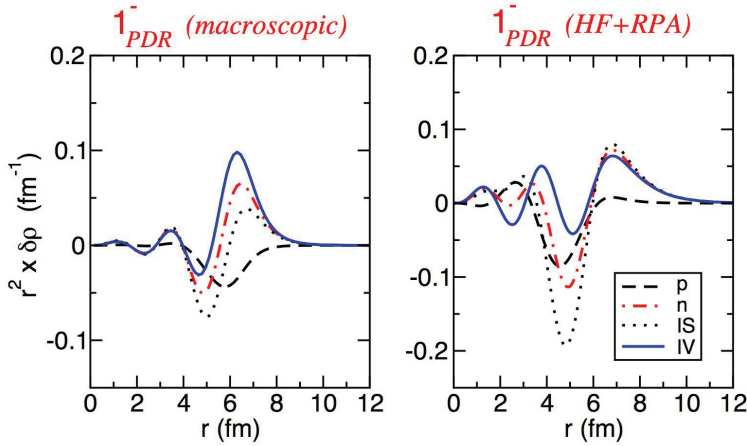


Figure 4. Transition densities for the low-lying dipole state for the ^{132}Sn isotope. The frame on the left show the macroscopic transition densities according to equations (2), the ones on the right are calculated microscopically with the HF + RPA with SGII interaction.

should also involve a collective nature of the state, which was not found to be fulfilled at least in our calculations.

3 Form Factors and Excitation of Dipole States via Coulomb and Nuclear Fields

As known [12], in the very-neutron rich nuclei the presence of different radii for the proton and neutron densities leads to non-vanishing isoscalar transition densities, opening the possibility of exciting the dipole states also via isoscalar probes. We want to explore the fact that a change in the reaction and in the bombarding energy, with the consequent change of the relative role of nuclear and Coulomb excitation processes, will alter the relative population of the different states.

The reaction mechanism is described according to the semiclassical model which assumes that nuclei move on classical trajectories, while the internal degrees of freedom are treated quantum mechanically [13]. These assumptions are known to be valid for grazing collisions. The Hamiltonian describing one of the colliding nuclei is formed by two parts: one describing the internal properties and the other is the external field responsible of the excitation of one partner of the reaction through the mean field of the other one. The Schrödinger equation is cast in a set of coupled equations for the probability amplitude of the states taken into consideration. Then the cross section for the excitation of each of the states is obtained by integrating the excitation probabilities over the impact parameter. More details are given in ref. [13].

The calculation includes the states with a strong EWSR percentage among the RPA ones. In order to reduce their number, we bunch together states with significant strength and whose energy is lying in a limited interval. The bunching is done by taking as energy the average energy of the states belonging to the group with the condition that the EWSR must be preserved. The dipole states so obtained and used in the calculations are shown in Table 1.

Table 1. Dipole states used in the calculations.

States	E (MeV)	EWSR %
1_{ll}^- (<i>PDR</i>)	9.3	1.1
1_{ll2}^-	11.3	4.4
<i>GDR</i>	13.9	56
1_{hl}^-	18.3	25

The real part of the nuclear optical potential, which together with the Coulomb interaction determines the classical trajectory, is constructed with the double folding procedure [14]. If we take into account also the isospin dependent part of the nucleon-nucleon interaction then the folding potential will be formed by

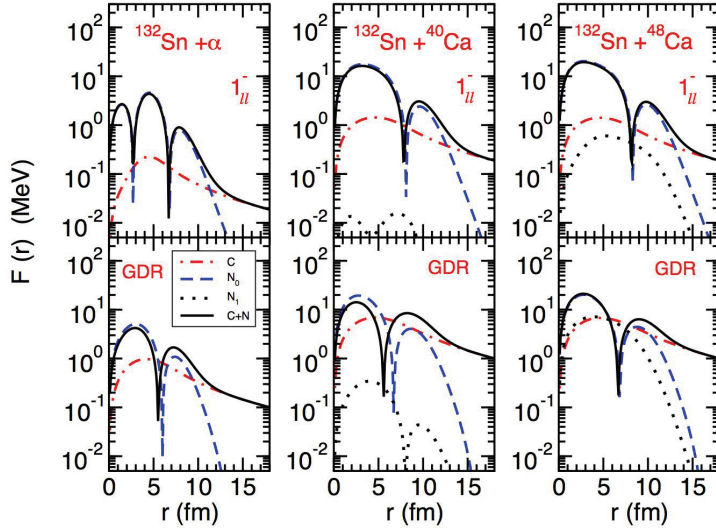


Figure 5. Formfactors for three different systems $^{132}\text{Sn} + \alpha$, ^{40}Ca , ^{48}Ca . The upper parts refer to the PDR states while the lower ones are for the GDR. The different component are shown together with the total one (solid black line).

two parts, one of them depending of the isospin degree of freedom. This part will go to zero when one of the two reaction partner has $N = Z$ [14].

The formfactors are obtained by double folding the transition densities from the ground states to the state in consideration with the density of the reaction partner and the isoscalar plus isovector nucleon nucleon interaction. Therefore, two components are obtained for the nuclear form factors. We will consider here the excitation of dipole states in ^{132}Sn by different partners: α , ^{40}Ca and ^{48}Ca . The formfactors for the PDR and GDR states are shown in Figure. 5. The nuclear components are indicated with dashed line (N_0 , the isoscalar part) and dotted line (N_1 , isovectorial part). We get strong contribution from the isovector part only for the ^{48}Ca case while in the other cases the contribution is inhibited because we have $N=Z$ for one of the reaction's partner. We note that the nuclear and Coulomb part interfere destructively at small radii and constructively at large radii. This is more evident for the GDR state and it is a direct consequence of the fact that the isoscalar dipole transition density has different sign at small and large radii [2, 15]. The interference is less pronounced in the ^{48}Ca case because of the presence of the isospin dependent part of the nuclear form factor. As a result, we expect that the GDR state will be less excited when the ^{48}Ca is used as a target rather than ^{40}Ca . Conversely, one is not expecting any change for the PDR state. Indeed, this can be seen in Figure 6 where the square of the nuclear and Coulomb formfactors, calculated at the surface, is reported as function of

Pygmy Dipole Resonances: Nuclear and Coulomb Excitations

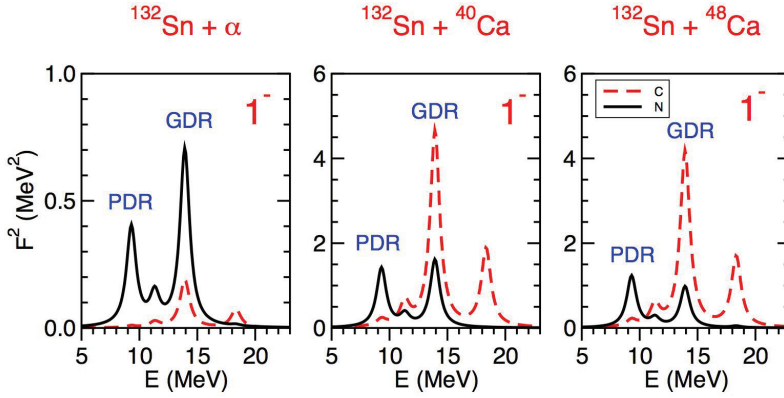


Figure 6. Square of the formfactor around the surface for different systems $^{132}\text{Sn} + (\alpha, ^{40}\text{Ca}, ^{48}\text{Ca})$. The distances around the surface have been taken at 7.7 fm, 11.0 fm and 11.3 fm for the three cases. Coulomb and nuclear contributions to the total formfactors are separately shown.

the excitation energy for the dipole states of Table 1. We already see at this level how different reactions may alter the relative intensities of the PDR and GDR states due to the different interplay of their isoscalar and isovector contributions.

This behaviour might be modified by the dynamics of the process. In Figure 7 we show the “partial wave cross section” for the system $^{132}\text{Sn} + ^{48}\text{Ca}$ at three different incident energies and for the two dipole states we are discussing, PDR and GDR. In the upper frames we notice that, independently of the incident energies, the Coulomb contribution for the GDR is always bigger than the PDR one. Conversely, the nuclear field (middle frames) produce a stronger excitation for the PDR. As the energy is decreasing, the relative strength of the excitation of the two states is going towards the same value as one can appreciate in the lower panels. We mention also that the nuclear contribution is generated by a small impact parameters range which should correspond to a small scattering angle range. Indeed, nuclear contributions are known to be enhanced at grazing angles, corresponding to “surface” impact parameters. An alternative possibility to balance the PDR and GDR excitations is to consider different partner reaction in order to alter the relative role of nuclear and Coulomb contributions. As an example, we show in Figure 8 the inelastic cross section for three different systems $^{132}\text{Sn} + (\alpha, ^{40}\text{Ca}, ^{48}\text{Ca})$ at the same incident energy (30 MeV/u). The Coulomb, nuclear contributions are separately shown as well as the total cross section. We should note that while at high bombarding energy the cross section is practically dominated by the one-step dipole component, at lower energies the dipole cross section might be embedded into a large background coming from other multipolarities or multistep excitations.

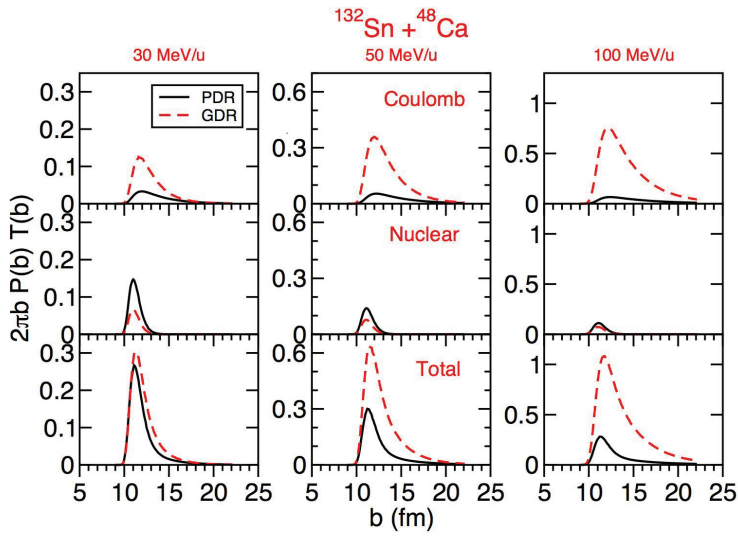


Figure 7. “Partial wave cross sections” vs. impact parameter b for the system $^{132}\text{Sn} + ^{48}\text{Ca}$. In each column are reported the results for the two dipole states, PDR and GDR, for three different incident energies. The upper part, the middle and the lower one show the results for the Coulomb, nuclear and total, respectively.

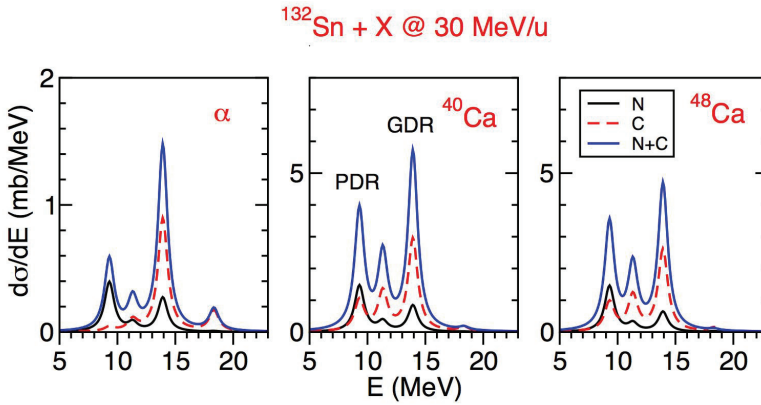


Figure 8. Differential cross sections as function of the excitation energy for the systems $^{132}\text{Sn} + \alpha$, ^{40}Ca , ^{48}Ca at 30 MeV per nucleon. Coulomb (dashed), nuclear (lower solid line) and total contributions are separately shown.

4 Summary

The nature of the PDR states has been analyzed within the H-F plus RPA formalism. We conclude that although they are formed by several particle hole config-

Pygmy Dipole Resonances: Nuclear and Coulomb Excitations

urations their collective nature may be questioned if one takes into account also the coherence properties. A detailed inspection of their transition densities reveals their strong isospin mixing allowing therefore the possibility to be excited also by an isoscalar probe even though their primary nature is isovector-like. We suggest then to use this feature in order to get valuable information on the nature of these states: Involving the nuclear interaction in the excitation processes together with the variation of the incident energy as well as the use of different combination of colliding nuclei one can disclose new features of these states.

References

- [1] N. Paar, D. Vretenar, E. Khan and G. Colò, *Rep. Prog. Phys.* **70** (2007) 691 and referencs therein.
- [2] F. Catara, E.G. Lanza, M.A. Nagarajan and A. Vitturi *Nucl. Phys. A* **614** (1997) 86; *Nucl. Phys. A* **624** (1997) 449.
- [3] P. Adrich *et al.*, *Phys. Rev. Lett.* **100** (2005) 132501; A. Klimkiewicz *et al.* (LANDFRS Collaboration), *Nucl. Phys. A* **788** (2007) 145; A. Klimkiewicz *et al.* (LAND Collaboration) *Phys. Rev. C* **76** (2007) 051603(R).
- [4] O. Wieland *et al.*, *Phys. Rev. Lett.* **102** (2009) 092502.
- [5] D. Savran *et al.*, *Phys. Rev. Lett.* **100** (2008) 232501.
- [6] J. Endres *et al.*, *Phys. Rev. C* **80** (2009) 034302.
- [7] A. Vitturi, E.G. Lanza, M.V. Andrés, F. Catara and D. Gambacurta, *PRAMANA* **75** (2010) 73.
- [8] E.G. Lanza, F. Catara, D. Gambacurta, M.V. Andrés and Ph. Chomaz, *Phys. Rev. C* **79** (2009) 054615.
- [9] D. Vretenar, N. Paar, P. Ring and G.A. Lalazissis, *Nucl. Phys. A* **692** (2001) 496.
- [10] G. Cò, V. De Donno, C. Maieron, M. Anguiano and A. M. Lallena *Phys. Rev. C* **80** (2009) 014308.
- [11] N. Tsoneva and H. Lenske, *Phys. Rev. C* **77** (2008) 024321.
- [12] J.A. Christley, E.G. Lanza, S.M. Lenzi, M.A. Nagarajan, and A. Vitturi, *J. Phys. G: Nucl. Part. Phys.* **25** (1999) 11.
- [13] E. G. Lanza, M.V. Andrés, F. Catara, Ph. Chomaz, M. Fallot and J. A. Scarpaci, *Phys. Rev. C* **74** (2006) 064614.
- [14] G. R. Satchler, *Direct Nuclear Reactions*, Oxford University Press 1983.
- [15] G.R. Satchler, *Nucl. Phys. A* **472** (1987) 215; S. Shlomo *et al.*, *Phys. Rev. C* **36** (1987) 1317; K.Nakayama and G. Bertsch, *Phys. Rev. Lett.* **59** (1987) 1053.